

Fungal Diversity (2013) 58:199–213
DOI 10.1007/s13225-012-0210-9

Stuck in time – a new *Chaenothecopsis* species with proliferating ascomata from *Cunninghamia* resin and its fossil ancestors in European amber

Hanna Tuovila · Alexander R. Schmidt ·
Christina Beimforde · Heinrich Dörfelt ·
Heinrich Grabenhorst · Jouko Rikkinen

Received: 15 June 2012 / Accepted: 15 October 2012 / Published online: 8 November 2012

© The Author(s) 2012. This article is published with open access at Springerlink.com

Abstract Resin protects wounded trees from microbial infection, but also provides a suitable substrate for the growth of highly specialized fungi. *Chaenothecopsis proliferatus* is described growing on resin of *Cunninghamia lanceolata* from Hunan Province, China. The new fungus is compared with extant species and two new fossil specimens from Eocene Baltic and Oligocene Bitterfeld ambers. The Oligocene fossil had produced proliferating ascomata identical to those of the newly described species and to other extant species of the same lineage. This morphology may represent an adaptation to growing near active resin flows: the proliferating ascomata can effectively rejuvenate if partially overrun by fresh, sticky exudate. Inward growth of fungal hyphae into resin has only been documented from Cenozoic amber fossils suggesting comparatively late occupation of resin as substrate by fungi. Still, resinicolous *Chaenothecopsis* species were already well adapted to their special ecological niche by the Eocene, and the morphology of these fungi has since remained remarkably constant.

Keywords Fossil fungi · Proliferating ascomata · Resin compounds · Ecology · Taxonomy

Introduction

Resinous exudates provide plants with protection against pathogens and parasites, but some highly specialized fungi are also known to grow exclusively on resin substrates. In the Mycocaliciales Tibell & Wedin (Eurotiomycetes, Ascomycota) some 10 % of the approximately 150 known species grow on plant exudates (Tibell and Titov 1995; Rikkinen 1999, 2003a; Titov 2006; Tuovila et al. 2011a, 2011b). Most of these fungi live on conifers and produce perennial, stipitate ascomata on hardened resin and/or resin-impregnated wood. Some species are also able to colonize relatively fresh, semisolid resin. The ability to rapidly exploit new substrates is advantageous, but also carries the inherent risk of being buried by subsequent resin flows. This danger is well exemplified, not only by the occurrence of partially or completely submerged ascomata in modern resins, but also by submerged specimens in European amber dating back to the Oligocene (Rikkinen and Poinar 2000) and Eocene (this study).

Here, we describe a new resinicolous *Chaenothecopsis* species from the exudate of *Cunninghamia lanceolata* (Lamb.) Hook. (Cupressaceae) from Hunan Province, China, as well as newly discovered *Chaenothecopsis* fossils from Eocene Baltic and Oligocene Bitterfeld ambers dating back to at least 35 and 24 Ma ago, respectively. The exquisite preservation of the fossils allows a detailed comparison with extant relatives. One fossil fungus has produced branched and proliferating ascomata similar to those of the newly described species from China, as well as some other extant species of the same lineage.

H. Tuovila · J. Rikkinen (✉)
Department of Biosciences, University of Helsinki,
P.O. Box 65, 00014 Helsinki, Finland
e-mail: jouko.rikkinen@helsinki.fi

A. R. Schmidt · C. Beimforde
Courant Research Centre Geobiology,
Georg-August-Universität Göttingen,
Goldschmidtstraße 3,
37077 Göttingen, Germany

H. Dörfelt
Mikrobielle Phytopathologie, Friedrich-Schiller-Universität Jena,
Neugasse 25, 07743 Jena, Germany

H. Grabenhorst
Nachtigallenweg 9,
29342 Wienhausen, Germany

Material and methods

Extant and fossil fungi

Resiniculous fungi were collected from tree trunks of *Cunninghamia lanceolata* (Cupressaceae), *Ailanthus altissima* (Mill.) Swingle (Simaroubaceae), *Kalopanax septemlobus* (Thunb.) Koidz (Araliaceae), and *Pinus massoniana* Lamb. (Pinaceae) in warm temperate evergreen broadleaved forests in Zhangjiajie National Forest Park in 1999, Badagongshan National Nature Reserve in 1999 and 2000, Daweishan National Forest Park in 2000, and Shunhuangshan National Forest Park in 2001 of Hunan Province in south-central China. For more information on the study area, see Koponen et al. (2000, 2004).

The fossils with proliferating ascocarps (Fig. 7) are preserved attached to wood debris in a 17×13×5 mm piece of Bitterfeld amber from the Heinrich Grabenhorst collection (collection number Li-83) that is now housed in the Geoscientific Collections of the Georg August University Göttingen (collection number GZG.BST.27285). Bitterfeld amber originates from the Goitzsche mine near the city of Bitterfeld (central Germany) and was recovered from the “Bernsteinschluff” Horizon in the upper part of the Cottbus Formation. The Upper Oligocene amber-bearing sediment has an absolute age of 25.3–23.8 Ma (Blumenstengel 2004; Knuth et al. 2002). A previous notion that Bitterfeld amber either represents re-deposited Eocene Baltic amber, or is at least much older than the amber-bearing strata (Weitschat 1997) was disproven by recent reconstructions of the sedimentary environment of this huge amber deposit (see Standke 2008, and discussion in Schmidt and Dörfelt 2007, and Dunlop 2010).

The non-proliferating fossil ascocarps (Figs. 8 and 9) are enclosed in a 2.5×1.5×1 cm piece of Baltic amber from the Jörg Wunderlich collection (collection number F1178/BB/FUN/CJW) that is now housed in the Geoscientific Collections of the Georg August University Göttingen (collection number GZG.BST.27286). Four immature and six mature ascomata derive from a mycelium that directly grew on the surface of a stalactite-like resin piece which served as substrate for the resinicolous fungus. These were preserved by a subsequent resin flow that had then covered over the material. The Eocene sediments containing the majority of Baltic amber in the Kaliningrad area (Russia) are 35–47 Ma old (Standke 1998).

Microscopy, imaging and microanalysis

Morphological features of the extant fungal specimens were observed and measured in water under a light microscope (Leica DMLS) with a 100x oil-immersion objective. Potassium-hydroxide (KOH), Lugol’s reagent (IKI), Melzer’s reagent (MLZ), Congo Red (CR; CR + congophilous, coloring

strongly red in CR), and nitric acid (N) were used when observing some diagnostic structures, like paraphyses and stipe hyphae. Ascomata from dried *Cunninghamia* bark pieces were imaged under a Carl Zeiss AxioScope A1 compound microscope using simultaneously incident and transmitted light. Spores were imaged on a microscope slide in water using 1600× (oil immersion) magnification and Differential Interference Contrast (DIC) illumination.

For scanning electron microscopy, several dried specimens of *C. proliferatus* were removed from the substrate, placed on a carbon-covered SEM-mount, sputtered by gold/palladium and examined under a Carl Zeiss LEO 1530 Gemini field emission scanning-electron microscope as described by Beimforde et al. (2011). Energy-dispersive X-ray spectroscopy (EDX) was performed on some ascomata using an INCA-EDX system (Oxford Instruments) with an excitation voltage of 15KV at this electron microscope.

The amber pieces were ground and polished manually with a series of wet silicon carbide abrasive papers to remove the weathered crusts and to minimize light scattering for the investigation. Prepared specimens were placed on a glass microscope slide with a drop of water applied to the upper surface of the amber, and covered with a glass coverslip. The inclusions were studied using a Carl Zeiss AxioScope A1 compound microscope. In most instances, incident and transmitted light were used simultaneously (see Schmidt et al. 2012, for protocols). In order to protect the amber from oxidation and breakage, the polished Baltic amber piece was embedded using polyester resin as described by Hoffeins (2001).

The images of Figs. 1, 2, 7, 8 and 9 (with exception of Figs. 2e, 7g, and 9f, g) are digitally-stacked photomicrographic composites obtained from several focal planes using the software package HeliconFocus 5.0 for a better illustration of the three-dimensional objects.

DNA extraction, PCR amplification and sequencing

DNA was extracted from extant representative specimens of resinicolous fungi collected from Hunan Province. Additional resinicolous, lignicolous and parasitic fungi were collected from different localities in Finland (2009) and northwestern USA (2006). DNA was extracted from 5 to 10 ascomata of each species with the NucleoSpin©Plant DNA extraction kit (Macherey-Nagel) with the following modification to the manufacturer’s protocol: specimens were incubated for 2 h to ensure the lysis of the ascocarps. The nuclear large subunit ribosomal RNA (LSU) partial gene was amplified using the primers LR0R and LR3 (Rehner and Samuels 1994; Vilgalys and Hester 1990). The ITS region of rDNA was amplified using the primers ITS4 and ITS5 (White et al. 1990) or alternatively ITS4 and ITS1F (Gardes and Bruns 1993). PCR amplification was conducted using Phusion® High-Fidelity DNA Polymerase (Thermo scientific/Finnzymes)



Fig. 1 Ascomata of *Chaenothecopsis proliferatus* sp. nov. on resin-impregnated bark of *Cunninghamia lanceolata* **a** Proliferating ascomata (JR 990048). **b** Multiple branching from capitulum (holotype, JR 990061). **c** Ascoma with branched stipe (holotype, JR 990061).

d Mature non-branched ascoma on resin (holotype, JR 990061). **e** Non-branched ascomata rising from a common stroma; note dense aerial mycelium (holotype, JR 990061). Scale bars: 200 μ m

according to the manufacturer's specifications using a 1:4 dilution of template DNA. PCR products were purified with GeneJET™ PCR Purification Kit (Fermentas). Amplicons were sequenced by Macrogen Inc. (South Korea) in the forward and reverse directions using the same primers as during amplification. Sequences for each sample were assembled into contigs using Geneious v5.4 (Drummond et al. 2011) and the consensus sequences used for further analyses. For samples that failed to amplify using the Phusion PCR method, amplification was conducted using PuReTaq Ready-To-Go PCR Beads (GE Healthcare, Piscataway NJ, USA) according to the manufacturer's instructions with the primers LROR & LR7 (Vilgalys and Hester 1990) or ITS1F & ITS4, and 3 μ L

of template DNA in a total PCR reaction volume of 25 μ L. These amplicons were then sequenced using an ABI 3100 automated sequencer (Applied Biosystems Inc., Foster City, CA, USA) with the primers ITS1F & ITS4, and LROR, LR3, LR5, and LR7.

Phylogenetic analyses

A concatenated dataset was composed of both the ITS and LSU sequences that were generated, and previous accessions from NCBI GenBank. The GenBank sequences were selected following two criteria: both ITS and LSU sequences were from the same voucher material (with the

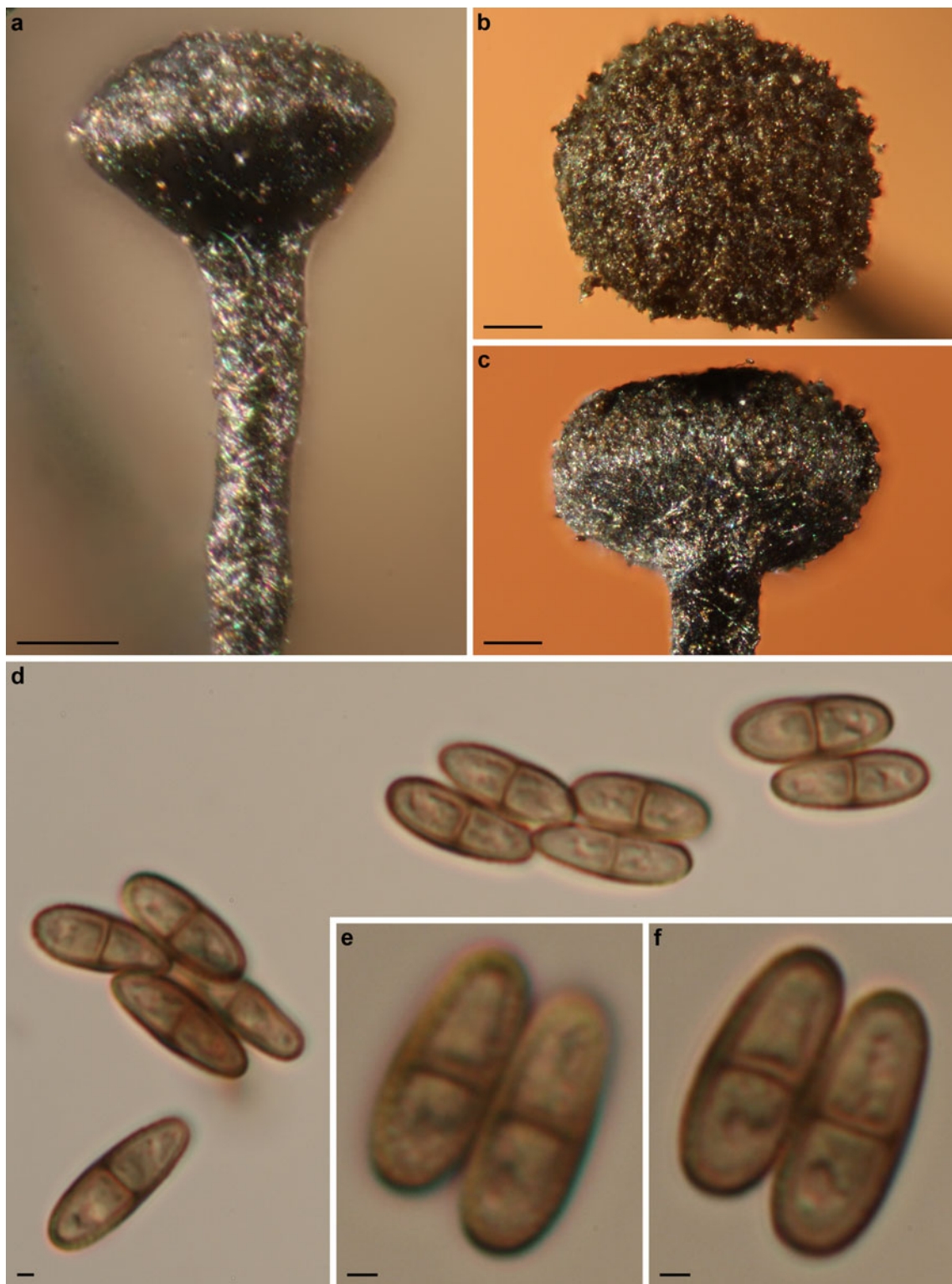


Fig. 2 Capitulum and spores of *Chaenothecopsis proliferatus* sp. nov. (holotype, JR 990061). **a** Young capitulum and upper section of stipe; note intertwined surface hyphae. **b** Capitulum with thin mazaedium

seen from above. **c** Exciple. **d** Ascospores. **e** Spore wall in focus. **f** Septum in focus. Scale bars: 50 μm (**a–c**) and 1 μm (**d–f**)

exception of *Mycocalicium sequoiae* from which only the LSU sequence was available), and sequences were from species with unequivocal taxonomic status. The dataset

was aligned with MAFFT version 6 (Kato and Toh 2008) and adjusted manually in PhyDE[®] 0.9971 (Müller et al. 2010). Unequivocal short (1–3 nucleotides) uninformative

insertions were first removed from the alignment, and the program Gblocks 0.91 (Castresana 2000) was then used to remove ambiguously aligned regions. Phylogenetic relationships and confidence statistics were inferred using a partitioned Bayesian approach in which models of evolution were generated independently with jModeltest 1.1 (Posada 2008) for each of the gene regions (LSU, ITS1, 5.8S, ITS2). The suggested evolutionary models (TIM2ef + G, HKY + G, TIM2ef + G, TIM3ef + G, respectively) were implied for the partitioned dataset.

Bayesian analyses were carried out with MrBayes 3.1.2 (Ronquist and Huelsenbeck 2003) on the freely available computational resource Biportal at the University of Oslo (<http://www.biportal.uio.no>; Kumar et al. 2009). Two independent runs, each with four chains, were conducted simultaneously for 10 million generations with trees sampled every 100th generation. Average standard deviations of split frequency (ASDSF) values lower than 0.01 were taken as an indication that convergence had been achieved. Five percent of the sampled trees were discarded as burnin and the remaining trees were used to estimate branch lengths and posterior probabilities. Additional support values were estimated using the same model parameters in Garli 2.0 for maximum likelihood (Zwickl 2006) with 1,000 bootstrap searchreps.

Voucher information and GenBank accession numbers of all fungal specimens used in this study are listed in Table 1.

Results

Extant fungus from China

Chaenothecopsis proliferatus Rikkinen, A. R. Schmidt et Tuovila **sp. nov.**

Figures 1, 2, 3, 4 and 5

Mycobank no.: MB800706

Type: China. Hunan Province. Dayong County, Zhangjiajie National Forest Park. Fuqiyuan, along trail to view point above Zhangjiajie Hotel; young mixed *Cunninghamia*-angiosperm forest with large remnant *Pinus massoniana*. On resin, resin-soaked bark, and lignum of *Cunninghamia lanceolata*. 15.IX.1999, 29°19'N, 110°25'E, elev. 650 m, Rikkinen JR990061 (holotype H).

Etymology: proliferatus refers to the common production of branched and proliferating ascocarps in this species.

Description

Apothecia on resin or resin-soaked wood and bark of *Cunninghamia lanceolata*, small to medium, 800–2,000 μm high, black with a bluish tinge. *Stipe* shiny black, long and slender, occasionally branching, 30–80 μm wide.

Capitulum discoid to lentil-shaped, rarely subspheric or ovoid, bluish black, 170–250 \times 300–400 μm . Young capitulum shiny, later spores accumulate as agglomerates on top of capitulum, appearing as black spots. Old capitulum covered with brown hyphae that possibly originate from germinated spores. New apothecia proliferate often from old capitula, usually several from the same capitulum. All parts of apothecium N– and MLZ–. *Asci* arise from croziers, cylindrical, 64.0–81.0 \times 3.5–4.5 μm ($n=10$), apex variously thickened and often penetrated by a short canal, mature asci sometimes without thickening. *Hymenium* and *hypothecium* IKI+, reaction fast and only seen by adding fresh IKI to a partly dried water squash preparation while observing through the microscope. The blue reaction usually disappears in seconds after the IKI has penetrated the material, the speed and the strength of the reaction seems to vary depending on the age and pigmentation of the ascocarp. *Ascospores* uniseriately and periclinally arranged, sometimes partly obliquely arranged in asci, brownish green, cylindrical to fusoid, one-septate, in mature spores septum as thick as spore wall, the spore wall inwardly thickened at junction between septum and spore wall; (7.2–) 7.5–11.3 (–11.8) \times 3.1–4.3 (–4.6); mean 10.3 \times 3.4 μm ($n=90$, from 9 ascocarps, 6 populations); $Q=1.9$ –3.6 μm , mean $Q=3.0$. Spores smooth under the light microscope, but each examined ascocarp typically had a small ratio (less than 15 %) of young spores with very minute, pointed ornamentation. *Paraphyses* hyaline, filiform, 65–85 \times 1.0–1.5 μm , occasionally branching from lower sections, commonly branching at the ascus tip level; septate, septal intervals 5.0–15.0 μm . Paraphyse tips covered with hyaline, strongly congophilous crystals that dissolve with KOH. *Hypothecium* hyaline to light green. *Exciple* green to brownish green in young apothecia, dark (greenish) brown in older ones, hyphae parallel, 3.0–4.0 μm wide, cell wall 0.5–1.5 μm , often with colorless crystals between and on top of hyphae of exciple, dissolving in KOH and MLZ; KOH + yellowish brown color leaks into medium and green pigments turn brown. Faint, but persisting grayish red to purplish pink IKI + reaction in thick-walled hyphae of exciple. Reaction is often difficult to observe due to the strong pigmentation of hyphal walls. *Stipe* dark green in young apothecia to dark brown in older ones, hyphae more or less parallel, partly intertwined, 3.0–5.0 μm wide, cell wall 1.5–2.0 μm , KOH + dark brown color leaks into medium and green colors of stipe turn brown. All parts of exciple and stipe covered with dense net of arching and horizontal hyphae 3.0 μm wide, cell wall 0.5–1.0 μm . *Epithecium* greenish to yellowish brown, composed of elements from exciple and paraphyses. The thick-walled hyphae of exciple cover the asci, intertwine and form a tight net that is hard to break, with small holes measuring 3.0 $\mu\text{m}\times$ 4.0 μm . Paraphyses curve at the level of ascus tips to cover the asci, branch repeatedly and anastomose with neighboring branches of the same and adjoining paraphyses just beneath the net of excipular hyphae,

Table 1 Voucher information and NCBI GenBank accession numbers for the fungal ITS and LSU sequences used in the study

Species	GenBank Accession numbers ITS/LSU	Reference ITS/LSU, if not same
<i>Pyrgillus javanicus</i> Nyl.	DQ826741/DQ823103	James et al. 2006
<i>Caliciopsis</i> sp.	GQ259981/GQ259980	Pratibha et al. 2011
<i>Chaenothecopsis consociata</i> (Násdv.) A.F.W.Schmidt	AY795851/DQ008999	Tibell and Vinuesa 2005
<i>Chaenothecopsis debilis</i> (Sm.) Tibell	AY795852/AY795991	Tibell and Vinuesa 2005
<i>Chaenothecopsis diabolica</i> Rikkinen & Tuovila	JX119109/JX119114	this study
<i>Chaenothecopsis dolichocephala</i> Titov	AY795854/AY795993	Tibell and Vinuesa 2005
<i>Chaenothecopsis fennica</i> (Laurila) Tibell	AY795857/AY795995	Tibell and Vinuesa 2005
<i>Chaenothecopsis golubkova</i> Tibell & Titov	AY795859/AY795996	Tibell and Vinuesa 2005
<i>Chaenothecopsis khayensis</i> Rikkinen & Tuovila	JX122785/HQ172895	this study/Tuovila et al. 2011a
<i>Chaenothecopsis montana</i> Rikkinen	JX119105/JX119114	this study
<i>Chaenothecopsis nigripunctata</i> Rikkinen	JX119103/JX119112	this study
<i>Chaenothecopsis proliferatus</i> Rikkinen, A.R.Schmidt & Tuovila	–/JX122783	this study
<i>Chaenothecopsis pusiola</i> (Ach.) Vain	JX119106/JX119115	this study
<i>Chaenothecopsis sitchensis</i> Rikkinen	JX119102/JX119111	this study
<i>Chaenothecopsis tsugae</i> Rikkinen	JX119104/JX119113	this study
<i>Chaenothecopsis vainioana</i> (Nádv.) Tibell	JX119107/JX119116	this study
<i>Chaenothecopsis viridireagens</i> (Násdv.) A.F.W.Schmidt	JX119108/JX119117	this study
<i>Chaenothecopsis pallida</i> Rikkinen & Tuovila (ined.)	JX122779/JX122781	this study
<i>Chaenothecopsis hunanensis</i> Rikkinen & Tuovila (ined.)	JR990061/JX122784	this study
<i>Chaenothecopsis resinophila</i> Rikkinen & Tuovila (ined.)	JX122780/JX122782	this study
<i>Chaenothecopsis</i> sp.	JX119110/JX119119	this study
<i>Phaeocalicium polypora</i> (Nyl.) Tibell ^a	AY789363/AY789362	Wang et al. 2005
<i>Mycocalicium sequoiae</i> Bonar	–/AY796002	Tibell and Vinuesa 2005
<i>Mycocalicium subtile</i> (Pers) Szatala	AF225445/AY796003	Vinuesa et al. 2001/Tibell and Vinuesa 2005
<i>Phaeocalicium populneum</i> (Brond ex Duby) A.F.W. Schmidt	AY795874/AY796009	Tibell and Vinuesa 2005
<i>Sphinctrina leucopoda</i> Nyl.	AY795875/AY796006	Tibell and Vinuesa 2005
<i>Sphinctrina turbinata</i> (Pers. ex Fr.) de Not	AY795877/DQ009001	Tibell and Vinuesa 2005
<i>Stenocybe pullatula</i> (Ach.) Stein	AY795878/AY796008	Tibell and Vinuesa 2005

^a Deposited as *Mycocalicium polypora* (Nyl.) Vain

forming an inner layer of the epithecium. This complex contains innumerable colorless, strongly congophilous crystals. Crystals also appear between paraphyses and asci, usually as a 15–20 µm thick layer. The crystals dissolve and green colors of epithecium turn brown in KOH. Faint, but persisting grayish red to purplish pink IKI + reaction in thick-walled hyphae of epithecium, usually difficult to observe due to the dark pigmentation of cell walls.

Specimens studied

China. Hunan Province. Resiniculous on basal trunk of *Cunninghamia lanceolata*. Dayong Co., Zhangjiajie National Forest Park. Dense mixed *Cunninghamia*-angiosperm forest along roadside in moist valley, 15.IX.1999. 29°19'N, 110°24'E, elev. 785 m, *Rikkinen*

JR990047 (UPS), *JR990048* (H). Moist evergreen forest with bamboo and conifer stands in valley below Zhangjiajie Hotel, 18.IX.1999, 29°19'N, 110°25'E. Elevation 630 m, *Rikkinen JR990312*, *JR990346* (SKLM). Yaozizhai, along lowest section of trail from valley bottom towards the peak, mature *Cunninghamia lanceolata* plantation along dry stream bed, 20.IX.1999, 29°18'N, 110°25'E, elev. 610 m, *Rikkinen JR990484*. Liu Yang Co., Daweishan National Forest Park. Xu-Quan Hu, low broadleaved secondary thickets with isolated *Cunninghamia lanceolata* in moist valley, 28.IX.2000, 28°25.30'N, 114°06.95'E, elev. ca. 1,300 m, *Rikkinen JR000470* (H). Lower section of trail from Li-Mu-Qiao to Wu-Zi-Shi crossing, secondary mixed evergreen forest with bamboo stands on steep slope of moist river valley, 28.IX.2000, 28°25.50'N, 114°05.35'E, elev. ca. 1,000 m,

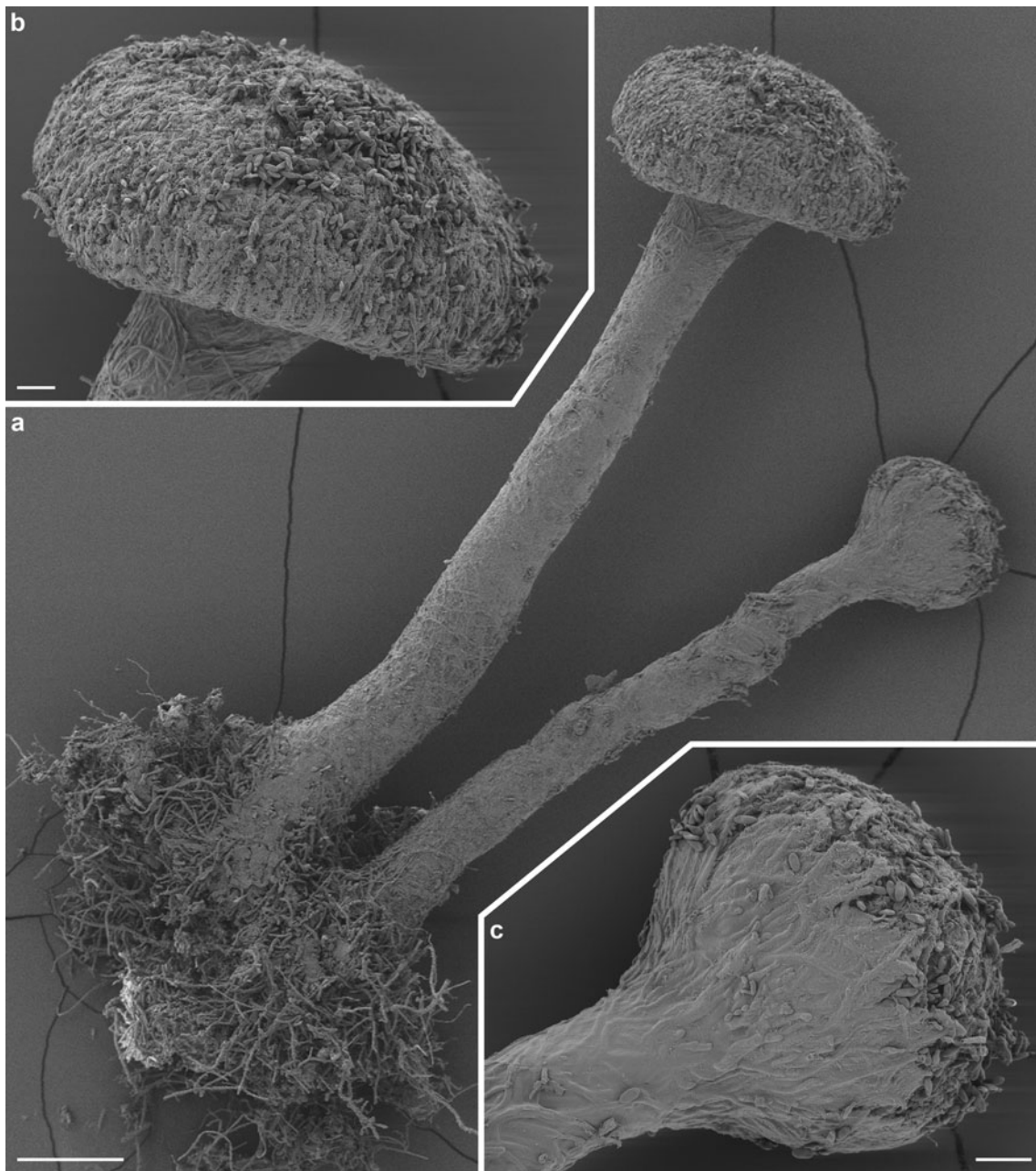


Fig. 3 SEM images of ascomata of *Chaenothecopsis proliferatus* sp. nov. (holotype, JR 990061). **a** Ascomata. **b** Detail of epithecium. **c** Detail of exciple. Scale bars: 100 µm (**a**) and 20 µm (**b** and **c**)

Rikkinen JR000594, JR000595 (H). Xinning Co., Shunhuangshan National Forest Park. Zheng Jiang Valley. *Cunninghamia lanceolata/Trachycarpus fortunei* stand in grazed mixed evergreen secondary forest, 24.IX.2001, 26°24' 35"N, 110°59'20" E, elev. 950 m, *Rikkinen JR010543* (H).

Phylogenetic analysis

The fungal LSU and ITS sequences obtained from extant *Chaenothecopsis* specimens in this study and from

GenBank were highly variable. There were no major indels in the LSU and 5.8S sequences, so these regions could be unambiguously aligned with Mafft. Conversely, the ITS1 and ITS2 sequences of most species had several apparently independent indels; in some cases tens of nucleotides long. Such unambiguous regions were removed before analysis. The lengths of sequences used in the phylogenetic analyses were: ITS1 137 bp (60 % of the original 227 positions), 5.8SR 155 bp (99 % of 156 positions), ITS2 130 bp (54 % of 238 positions), and partial LSU 534 bp (97 % of 548

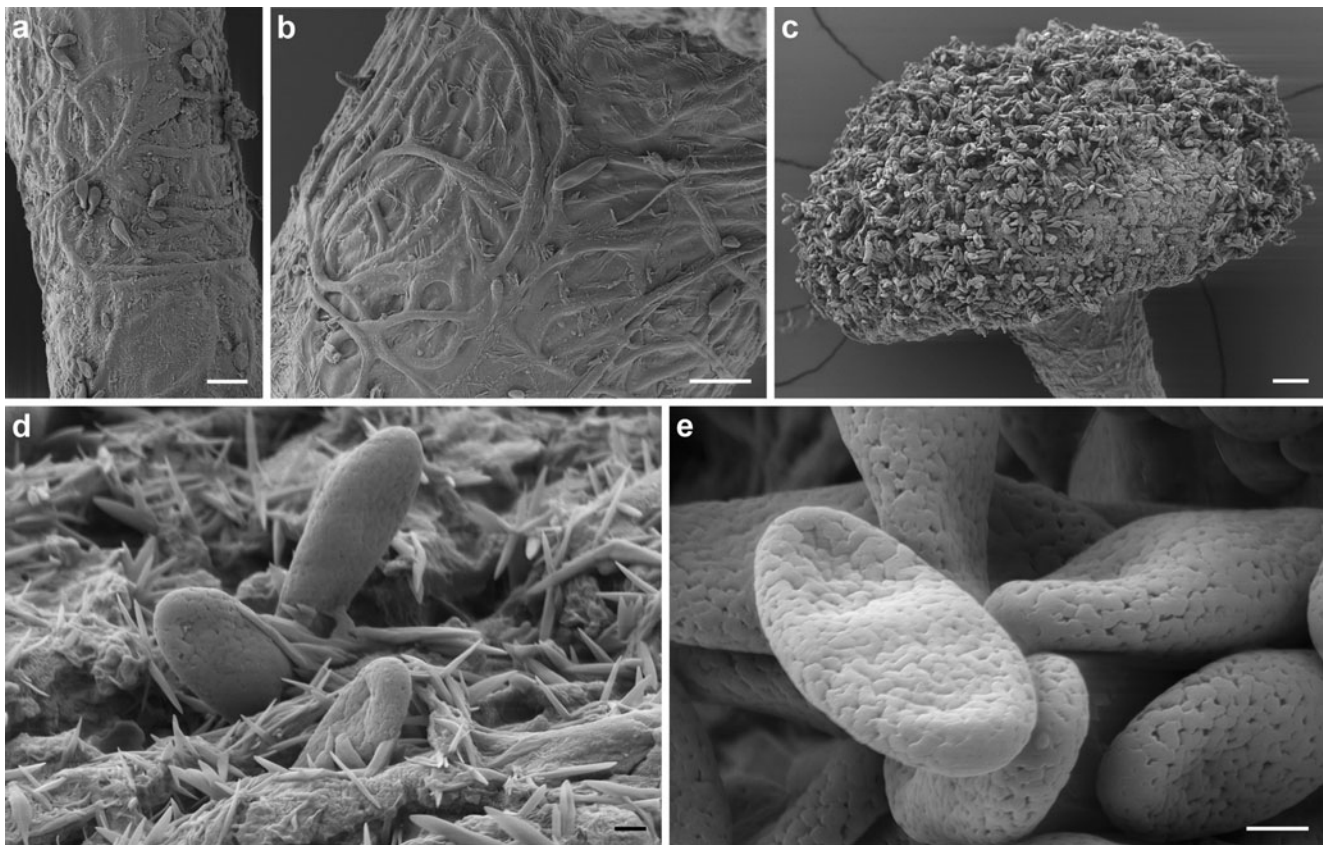


Fig. 4 SEM images showing anatomical details of *Chaenothecopsis proliferatus* sp. nov. (holotype, JR 990061). **a** Stipe surface. **b** Stipe surface near exciple. **c** Epithecium. **d** Ascospores being released

through the epithecium; note the blade-like crystals. **e** Ascospores. Scale bars: 10 μm (**a** and **b**), 20 μm (**c**) and 1 μm (**d** and **e**)

positions). The resulting alignment has been uploaded to TreeBase, direct accession: <http://purl.org/phylo/treebase/phyloids/study/TB2:S12780>.

The results of the phylogenetic analysis are shown in Fig. 6. The phylogeny is broadly consistent and adds to the previous results of Tibell and Vinuesa (2005) and Tuovila et al. (2011a). It places *C. proliferatus* in the same clade with several other *Chaenothecopsis* species with one-septate spores. This clade includes taxa that grow on conifer resins, a species that grows on conifer lignum, and several species that are either lichen-parasitic or associate with free-living green algae.

Chaenothecopsis proliferatus and the closely related *C. humanesis* Rikkinen & Tuovila (ined.) had a negative effect on the posterior probabilities of the tree. If these species were removed from the dataset, the other species showed qualitatively similar groupings with higher posterior probabilities (tree not shown). This is probably explained by the fact that only LSU sequences were available for these two new species from China; presumably due to the relatively old age of the specimens (over 10 years), we were not able to amplify ITS sequences from them. Without information from ITS sequences, there is a level

of uncertainty regarding the exact placement of these two taxa within their clade. In an analysis based solely on LSU sequences, the sister group relationship between the four lichen-parasitic taxa and the clade of *C. dolichocephala*, *C. sitchensis* and *C. fennica* gained higher support, but the placement of *C. proliferatus* remained unresolved (tree not shown).

Fossil specimens from European amber

Amber piece GZG.BST.27285 (Bitterfeld amber) contains fossilized remains of over 45 stipitate fungal ascomata (Fig. 7a–b). These represent different developmental stages from young initials to mature and senescent ascomata. Individual ascomata erect, 250–1100 μm high, forming stacks of up to three ascomata of different ages by proliferating and branching (Fig. 7a–c). Exciple well-developed, smooth, with partly intertwined surface hyphae (Fig. 7d–e). Stipe slender, 30–80 μm in diameter, smooth, with partly intertwined hyphae (Fig. 7b–d). Tufts of anchoring hyphae penetrate the substrate (Fig. 7a–b). Ascospores narrowly ellipsoidal to cylindrical, one-septate, 9–10.5 \times 3.5–4.5 μm , appearing smooth under the light microscope (Fig. 7f–g).

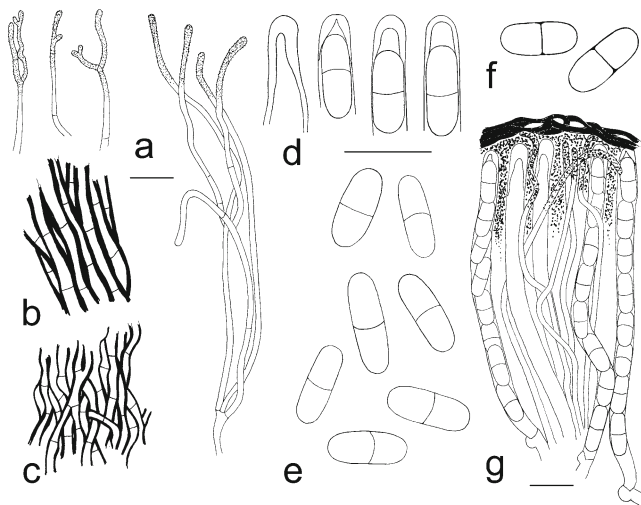


Fig. 5 Line drawings of anatomical details of *Chaenothecopsis proliferatus* sp. nov. (in water and CR). **a** Paraphyses (JR990346, JR000595). **b** Stipe (JR990048). **c** Exciple (JR990048). **d** Ascus tip (JR990061, JR000595). **e** Ascospores (JR990048, JR990061, JR990312, JR000595). **f** Spore wall (JR990312). **g** Paraphyses, asci, and epithecium (JR000593). Scale bars: 10 μm. Drawing by HT

Amber piece GZG.BST.27286 (Baltic amber) contains fossilized remains of at least 15 stipitate fungal ascomata (Fig. 8a). These include ten well-preserved ascomata (4 immature, 6 mature) and at least five degraded ascomata. Many details not visible due to weathered crust around the latter inclusions. Ascomata erect and non-branching, 1,500–1,840 μm high when mature (Figs. 8a, 9a). Immature, developing ascomata with sharply pointed apices (Fig. 9b–c). Capitula lenticular to subhemispheric, 260–380 μm wide and 120–200 μm high, with a well-developed exciple (Fig. 9a). Mature ascospores have accumulated on top of epithecium (Fig. 9d). Stipe long and rather robust, 90–160 μm in diameter, smooth or with a somewhat uneven surface of partly intertwined hyphae. (Fine details not visible due to thin film of air around the inclusions) (Fig. 9a–e). Tufts of anchoring hyphae attach the ascomata to the substrate (Fig. 9a–b) and penetrate deeply into the resin (Fig. 8b–c). Ascospores narrowly ellipsoidal to cylindrical, one-septate, 8–11 × 3–4 μm, appearing smooth under the light microscope (Fig. 9f–g).

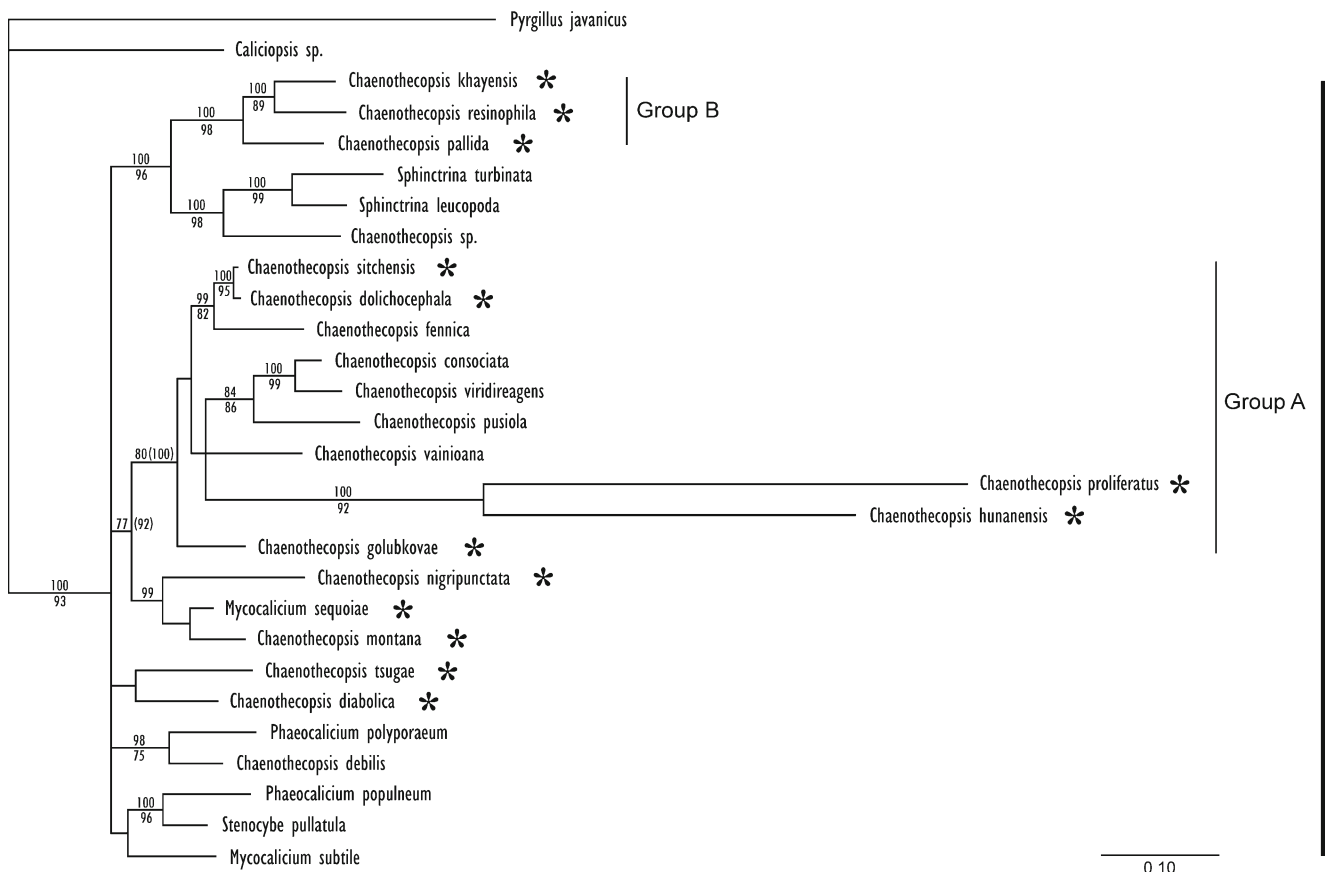


Fig. 6 Phylogenetic relationship of *Chaenothecopsis proliferatus* based on analysis of ITS and partial LSU sequences. Support values are indicated for nodes that received support from at least one method (Bayesian posterior probabilities shown above the nodes; maximum-likelihood bootstrap values shown below the nodes). *Chaenothecopsis proliferatus* and *C. hunanensis* had a negative effect on the posterior

probabilities of the tree. The values in parenthesis refer to posterior probabilities when these two species were not included in the analysis. The clade corresponding to the Mycocaliciales is shown by a vertical bar, and the resinicolous species are indicated by an asterisk. Group A species with one-septate ascospores. Groups B species with aseptate ascospores from angiosperm exudates

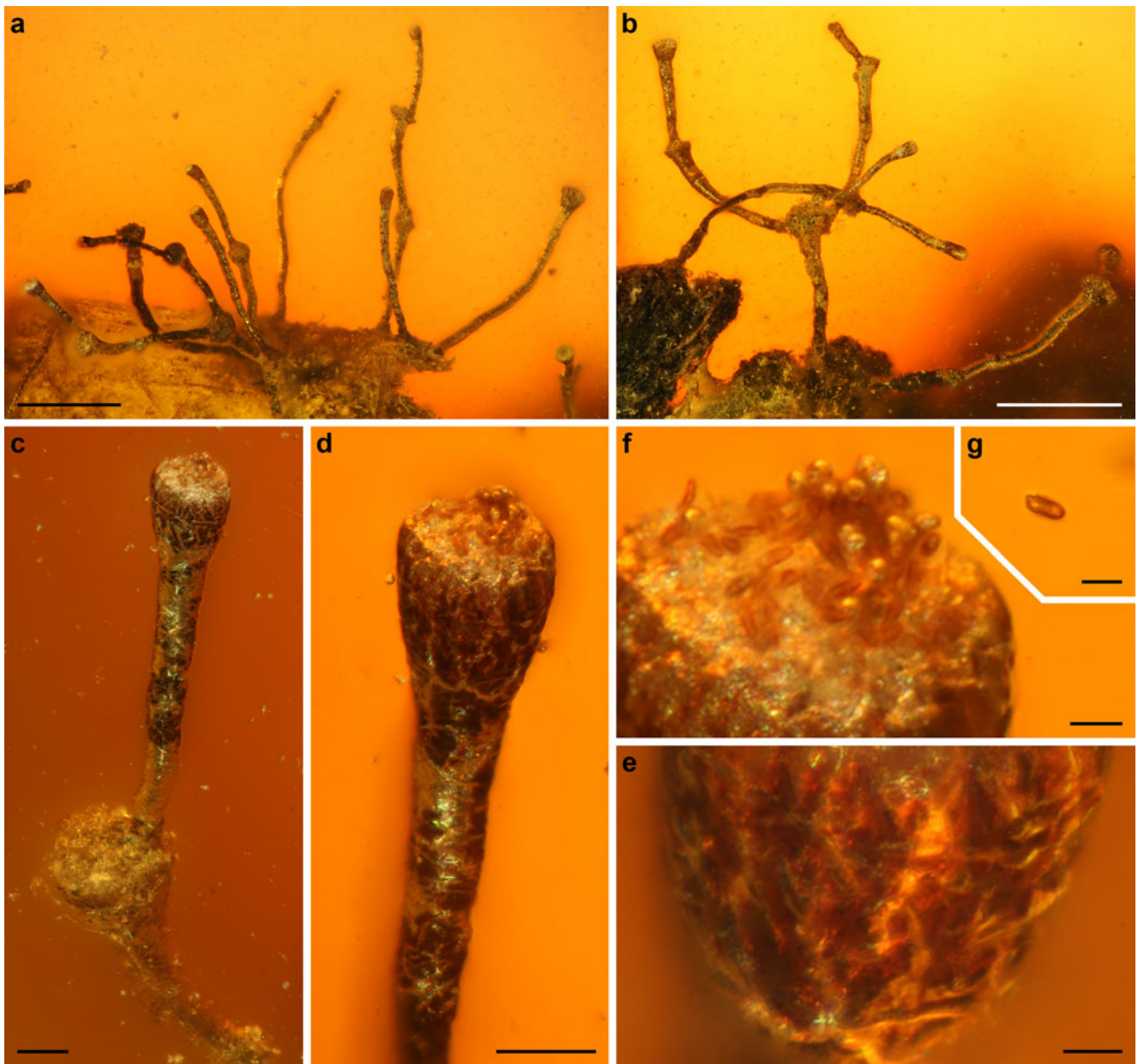


Fig. 7 Fossil *Chaenothecopsis* from Bitterfeld amber (GZG.BST.27285). **a–b** Proliferating ascomata. **c–d** Young ascoma. **e** Exciple. **f** Epithecium, note the accumulated ascospores. **g** Detached ascospore. Scale bars: 500 μm (**a** and **b**), 50 μm (**c** and **d**) and 10 μm (**e–g**)

Discussion

Taxonomy and evolutionary relationships

In their substrate ecology, general morphology, and in the production of septate ascospores, *Chaenothecopsis proliferatus* and the two newly described fossils closely resemble each other, as well as several other *Chaenothecopsis* species from Eurasia and western North-America. The phylogenetic analyses indicate that *C. proliferatus* is closely related to previously known species that live on conifer resin and have one-septate ascospores (Group A in Fig. 6). In as much as

both fossils had produced similar spores, and because Baltic and Bitterfeld ambers are fossilized conifer resins, these fossils are likely to belong to this same lineage. No *Chaenothecopsis* species with aseptate spores were included in this lineage, and the phylogenetic analysis grouped three such species from angiosperm exudates into a different well-supported clade (Group B in Fig. 6), as a sister group to the two *Sphinctrina* species.

As the substrate preferences of Mycohaliciales are highly specialized, and spore septation is an important taxonomic character, only resinicolous *Chaenothecopsis* species with one-septate ascospores are here compared with *C.*

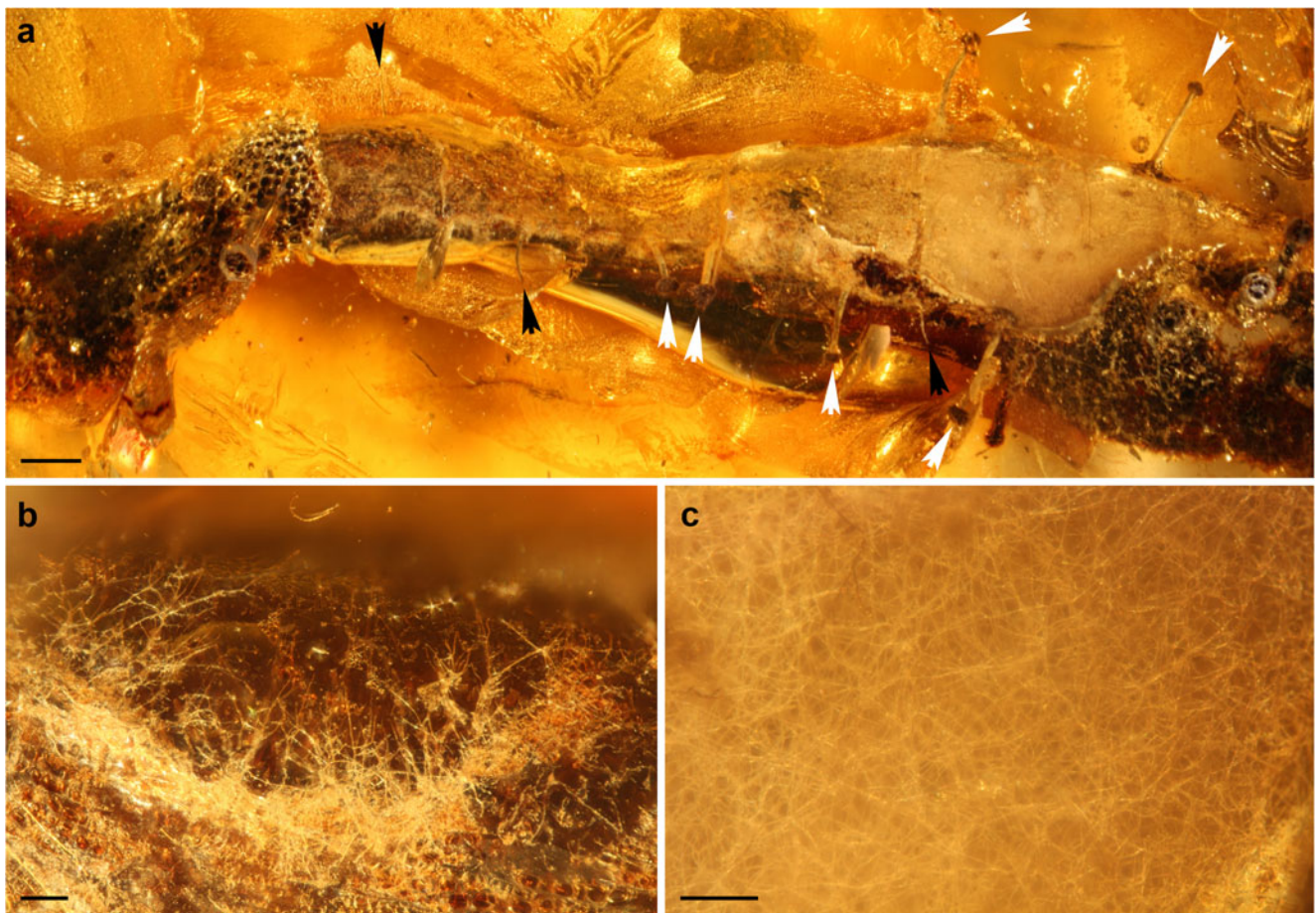


Fig. 8 Overview of the fossil *Chaenothecopsis* from Baltic amber (GZG.BST.27286). **a** Ascomata on a stalactite-like piece of solidified resin which was subsequently covered by fresh exudate. *Black arrowheads* point to young developing ascomata, *white arrowheads* to

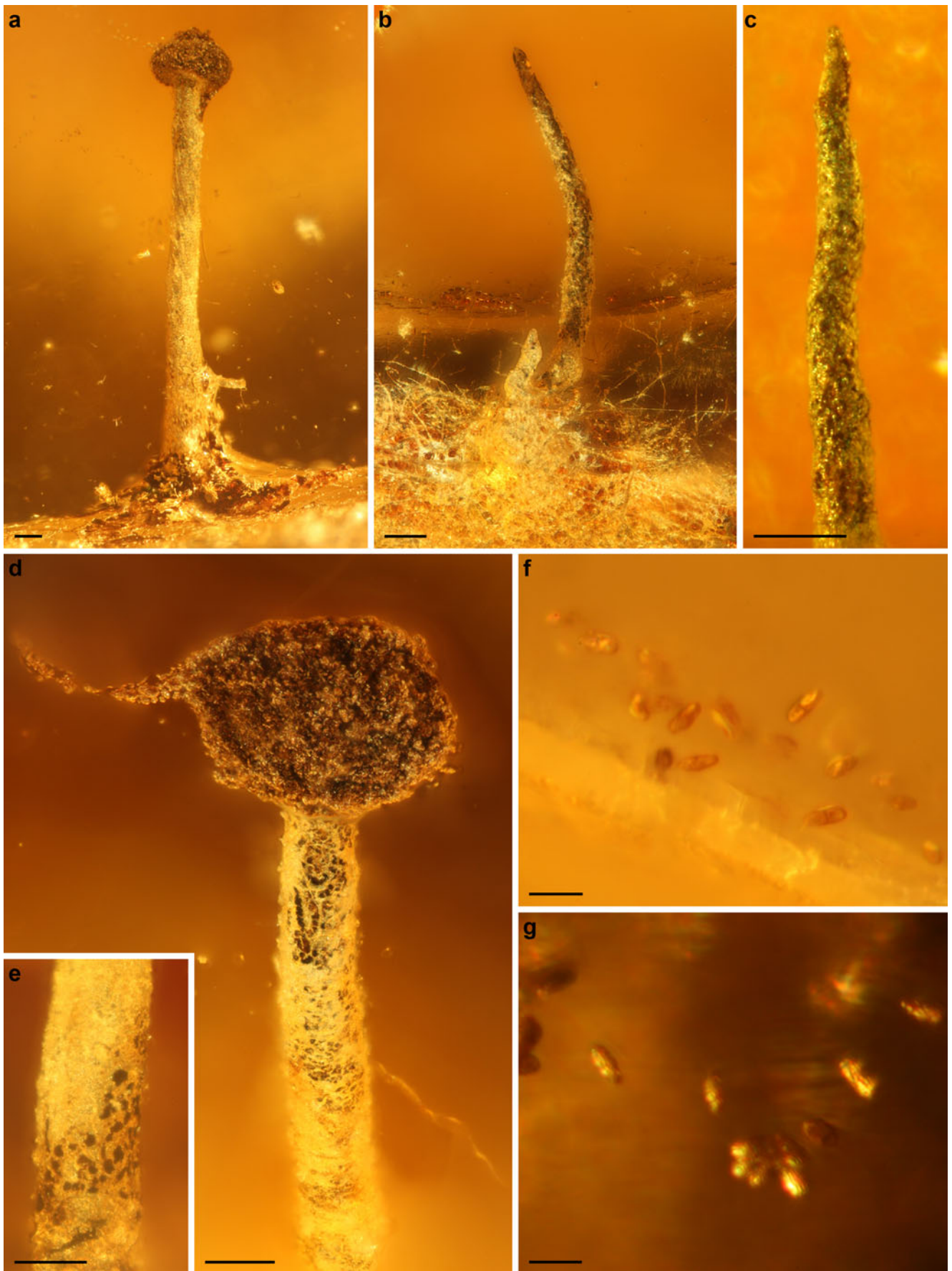
mature ascomata. **b** Fungal hyphae that grew on and into the stalactite-like resin substrate before it solidified. **c** Dense mycelium on the old resin flow. Scale bars: 1 mm (**a**) and 100 μ m (**b** and **c**)

proliferatus and the two fossils. *Chaenothecopsis sitchensis* Rikkinen, *C. nigripunctata* Rikkinen, and *C. edbergii* Selva & Tibell grow on conifer resin in temperate North America and often produce large and robust ascocarps. *C. sitchensis* lacks the fast IKI + reactions typical of *C. proliferatus* and has distinctively ornamented ascospores (Rikkinen 1999). *C. nigripunctata* has larger spores than *C. proliferatus* and a highly distinctive appearance due to its gray, compound capitula (Rikkinen 2003b). *C. edbergii* differs from *C. proliferatus* in having a persisting blue MLZ + reaction in the hymenium and a lime green pruina on the surface of its ascomata (Selva and Tibell 1999).

Compared to *Chaenothecopsis proliferatus*, *C. eugenia* Titov (Titov 2001) and *C. asperopoda* Titov (Titov and Tibell 1993) both have smaller spores, very thin septa and a diagnostic stipe structure and coloration. These two species appear to be closely related, but unfortunately we were unable to extract sufficient DNA for sequencing, presumably due to the old age (ca. 20 years) of the type material. Both species have a fast blue IKI + reaction of the

hymenium and an IKI + red reaction of stipe similar to *C. proliferatus*. The latter color reaction is more easily observed in these species than in *C. proliferatus* because their stipes are less pigmented.

Chaenothecopsis dolichocephala (Tibell and Titov 1995), *C. golubkovae* (Titov and Tibell 1993) and *C. hunanensis* are very similar to *C. proliferatus*. *C. dolichocephala* often produces branched and proliferating fruiting bodies, has similar colorless crystals in the hymenium, and also shares a similar anatomy of the stipe and exciple. However, its ascomata are on average smaller, the stipe is shinier and the ascospores are ornamented. The blue IKI + reaction is very faint or non-existing and the red IKI + reaction occurs only in the lower part of exciple and stipe, if at all. The spore size, epithelial structure and the IKI + color reactions of *C. golubkovae* are more or less identical to those of *C. proliferatus*. However, *C. golubkovae* is characterized by the highly branched and irregularly shaped hyphae (textura epidermoidea) formed from fused cell walls of the exciple and stipe. *C. hunanensis* has slightly smaller spores with



◀ **Fig. 9** Ascomata and anatomical details of the fossil *Chaenothecopsis* from Baltic amber (GZG.BST.27286). **a** Mature ascoma. **b** Young, developing ascoma and fungal mycelium. **c** Tip of developing ascoma (compare with Fig. 25 in Rikkinen 2003a). **d** Capitulum and upper part of stipe; note the accumulated ascospores. Numerous abscised spores extend into the amber matrix in the upper left. **e** Closer view of stipe surface. **f–g** Detached ascospores. Scale bars: 100 μm (**a–e**) and 10 μm (**f** and **g**)

thin septa and a different type of epithecium when compared with *C. proliferatus*.

The distinction between *C. proliferatus*, *C. dolichocephala*, *C. golubkova* and *C. hunanensis* requires study of anatomical details and chemical features that cannot be observed from fossil specimens embedded in amber. Hence, despite their excellent preservation, we do not want to assign the new fossils to any extant species, and we also refrain from assigning them to the previously described *Chaenothecopsis bitterfeldensis* Rikkinen & Poinar. However, the four extant species and the three fossils are obviously closely related and most probably belong to the same lineage since *C. bitterfeldensis* resembles *C. proliferatus* and the two newly discovered fossils in ecology and spore type (Rikkinen and Poinar 2000).

The morphological similarities between *C. proliferatus* and the proliferating fossil from Bitterfeld amber are especially striking. The only obvious difference is in the size of the fruiting bodies, with the preserved ascocarps of the fossil being distinctly smaller than typical ascocarps of *C. proliferatus*. Both fungi have relatively slender, commonly branched and proliferating fruiting bodies. The shape and general appearance of the capitula of young fruiting bodies are also identical. The stipes of both fungi are lined by a net of arching and horizontal hyphae (compare Figs. 2a, c and 7d, e), and these hyphae extend to the epithecium in a similar way. In both fungi, the one-septate and smooth (or minutely punctate) ascospores accumulate on top of the epithecium. All these morphological features together indicate that the fossil is closely related to *C. proliferatus*.

The epithecium of *Chaenothecopsis proliferatus* is, in places, covered by a thin layer of small crystals. These blade-like structures are typically 1–3 μm long and sharply pointed at both ends (Fig. 4d). While some crystals seem to be partly embedded in the extracellular matrix of fungal hyphae, most appear external. Similar crystals are also present on the upper section of the stipe (Fig. 4b). In their general appearance, the crystals somewhat resemble the needle-like calcium oxalate crystals that cover the hyphal surfaces of some fungi. Such crystals are formed when oxalic acid secreted by the fungus combines with external calcium to produce calcium oxalate (Dutton and Evans 1996). However, only carbon and oxygen were detected from the epithecium surface of *C. proliferatus* in EDX analyses.

Occurrence and ecological role of proliferating ascocarps

The ascomata of many species of Mycocaliciales can occasionally have a capitulum in which the apothecial disk is divided into several distinct regions or lobes. Asci tend to first mature in the central sections of the hymenia and when more asci mature, the hymenium expands and the capitulum surface become increasingly convex. Irregularities in ascus production can easily lead to the development of several hymenial convexities or lobes per capitulum. Many *Chaenothecopsis* species can also occasionally produce branched ascocarps, and these structures appear to be especially common in resinicolous species with long and slender stipes, such as *C. oregana* Rikkinen and *C. diabolica* Rikkinen & Tuovila. However, ascocarp braching is not confined only to resinicolous species, but also occurs in some lichen-associated and lignicolous species such as *C. haematopus* Tibell and *C. savonica* (Räsänen) Tibell, which typically grow on lignum in shaded microhabitats. Branching also occurs in some species of *Mycocalicium* Vain., *Phaeocalicium* A.F.W. Schmidt and *Stenocybe* Nyl. ex Körb. For example, *Stenocybe pullatula* (Ach.) Stein can produce several capitula from the same stipe, with the youngest at the tip and the older, senescing capitula appearing as a whorl directly below. This species produces ascocarps on the bark of *Alnus* species.

In the resinicolous *Chaenothecopsis nigripunctata* branching mainly occurs very close to the tip of the stipe, with each short branch forming a separate apothecial head. Profuse branching often leads to the development of compound capitula, consisting of up to twelve partially contiguous apothecial heads (Rikkinen 2003b). *Mycocalicium sequoiae* Bonar also produces clusters of apothecial heads on a common stipe (Bonar 1971). However, in this species the stipes tend to branch lower and hence have longer branches and less confluent apothecial heads than in *C. nigripunctata*. Also the related *C. montana* Rikkinen can produce branched ascocarps, but more rarely than the other two species (Tuovila et al. 2011b).

While the ascomata of *C. nigripunctata* and its closest relatives mainly branch from the upper part of the stipe, their ascocarps do not usually form multi-layered groups via branching and proliferation through the hymenium in the way exhibited by the proliferating fossil from Bitterfeld amber and many specimens of *C. proliferatus*. However, similar branching is quite common in the resinicolous *C. dolichocephala* and *C. sitchensis*, both of which usually have very narrow and long stipes. This shared morphology might represent an adaptation to growing near active resin flows: the perennial ascocarps can effectively rejuvenate in situations where they happen to be partly submerged in fresh exudate. All three species commonly live on cankers and wounds which exude resin over extended periods.

It seems unlikely that the ascomata of resinicolous *Chaenothecopsis* species could rejuvenate after being rapidly and completely submerged in fresh sticky resin. Even the fossil specimens had first produced fruiting bodies on hardened resin and then had subsequently been covered by a thick layer of fresh exudate. This raises the question of what then triggers the proliferation in partly submerged ascocarps and those ascocarps only growing close to fresh resin. It has been shown that some fungi react to the volatile compounds produced by other fungi when competing for resources (Evans et al. 2008). It is also known that fresh resin contains high levels of volatile compounds, mainly monoterpenes and sesquiterpenes, when compared to older, semisolid exudate, and that the hardening of resin is directly related to the loss of such compounds (e.g. Langenheim 2003; Ragazzi and Schmidt 2011). An ability to detect and respond to the presence of volatile resin compounds in the environment would give the *Chaenothecopsis* species time to prepare for a potential burial in freshly exuding resin. It seems feasible that some resinicolous fungi could begin to branch when the concentration of volatile resin compounds in their typically sheltered microenvironment is sufficiently high as to indicate that a fresh resin flow may be imminent. In other fungi the differentiation of fruiting bodies is commonly triggered by the perception of some change in environmental conditions, such as light, pH, oxygen etc. (Busch and Braus 2007).

The hyphae of extant resinicolous fungi commonly penetrate and grow into semisolid resin. Evidence of inward growth of fungal hyphae is also preserved in numerous worldwide amber fossils since the Paleocene (personal observation), but no evidence of a similar capability has yet been found prior to the Cretaceous-Paleogene boundary. Cretaceous amber pieces from several different deposits may contain abundant filaments that grew from the resin surface into liquid resin, but all of these have been identified as filamentous prokaryotes (see Schmidt and Schäfer 2005; Schmidt et al. 2006; Girard et al. 2009a, b; Beimforde and Schmidt 2011), not as fungal hyphae. This suggests that this special niche was either occupied by prokaryotes in the Mesozoic or that *Chaenothecopsis* species (if already existent) and other ecologically similar fungi did not yet exploit resin substrates.

Conclusions

Fossil evidence of inward growth of fungal hyphae into plant exudates has not been identified from Mesozoic ambers, suggesting a relatively late occupation of such substrates by ascomycetes. Even so, resinicolous *Chaenothecopsis* species were well adapted to their niche by the Eocene and the ecology and morphology of these fungi has since remained

unchanged. The Oligocene fossil had produced proliferating ascomata identical to those of the newly described species from China and its extant relatives. This morphology may represent an adaptation to life near exuding resin: the proliferating ascomata can effectively rejuvenate if partly overrun by fresh exudate. While many extant *Chaenothecopsis* species live on lichens and/or green algae, the fossils and the sporadic occurrence of resinicolous taxa in several distantly related extant lineages suggests that the early diversification of Mycocaliciales may have occurred on plant substrates.

Acknowledgments The field work in Hunan Province was done in cooperation with the Forestry Department of Hunan Province and its Forest Botanical Garden, and the Department of Biosciences (formerly Department of Ecology and Systematics), and the Botanical Museum, University of Helsinki. We thank Timo Koponen who's Academy of Finland project (no 44475) made the field work possible. Jörg Wunderlich (Hirschberg and der Weinstraße, Germany) kindly provided an amber piece of his collection for this study and Hans Werner Hoffeins (Hamburg) embedded the Baltic amber piece in polyester resin. We are grateful to Eugenio Ragazzi (Padova) for discussion about resin chemistry, to Dorothea Hause-Reitner (Göttingen) for assistance with field emission microscopy and to Leyla J. Seyfullah (Göttingen) for comments on the manuscript. Marie L. Davey (University of Oslo) provided indispensable help with sequencing difficult samples and advice on the molecular work. The work of H.T. was supported by research grants from the Jenny and Antti Wihuri Foundation and Ella and Georg Ehrnrooth Foundation. This is publication number 92 from the Courant Research Centre Geobiology that is funded by the German Initiative of Excellence.

Open Access This article is distributed under the terms of the Creative Commons Attribution License which permits any use, distribution, and reproduction in any medium, provided the original author(s) and the source are credited.

References

- Beimforde C, Schmidt AR (2011) Microbes in resinous habitats: a compilation from modern and fossil resins. *Lect Notes Earth Sci* 131:391–407
- Beimforde C, Schäfer N, Dörfelt H, Nascimbene PC, Singh H, Heinrichs J, Reitner J, Rana RS, Schmidt AR (2011) Ectomycorrhizas from a Lower Eocene angiosperm forest. *New Phytol* 192:988–996
- Blumenstengel H (2004) Zur Palynologie und Stratigraphie der Bitterfelder Bernsteinvorkommen (Tertiär). *Exkursionsführer und Veröffentlichungen der Deutschen Gesellschaft für Geowissenschaften* 224:17
- Bonar L (1971) A new *Mycocalicium* on scarred *Sequoia* in California. *Madrono* 21:62–69
- Busch S, Braus GH (2007) How to build a fungal fruit body: from uniform cells to specialized tissue. *Mol Microbiol* 64:873–876
- Castresana J (2000) Selection of conserved blocks from multiple alignments for their use in phylogenetic analysis. *Mol Biol Evol* 17:540–552
- Drummond AJ, Ashton B, Buxton S, Cheung M, Cooper A, Duran C, Field M, et al. (2011) Geneious v5.4. Retrieved from www.geneious.com 1 May 2011
- Dunlop J (2010) Bitterfeld amber. In: Penney D (ed) *Biodiversity of Fossils in Amber*. Siri Scientific Press, Manchester, pp 57–68

- Dutton MV, Evans CS (1996) Oxalate production by fungi: its role in pathogenicity and ecology in the soil environment. *Can J Microbiol* 42:881–895
- Evans JA, Eyre CA, Rogers HJ, Boddy L, Müller CT (2008) Changes in volatile production during interspecific interactions between four wood rotting fungi growing in artificial media. *Fungal Ecol* 1:57–68
- Gardes M, Bruns TD (1993) ITS primers with enhanced specificity for basidiomycetes—application to the identification of mycorrhizae and rusts. *Mol Ecol* 2:113–118
- Girard V, Breton G, Brient L, Neraudeau D (2009a) Sheathed prokaryotic filaments, major components of mid-Cretaceous French amber microcoenoses. *J Paleolimnol* 42:437–447
- Girard V, Schmidt AR, Struwe S, Perrichot V, Breton G, Neraudeau D (2009) Taphonomy and palaeoecology of mid-Cretaceous amber-preserved microorganisms from southwestern France. In: Perrichot V, Neraudeau D (eds) *Cretaceous ambers from southwestern France: geology, taphonomy, and palaeontology*. *Geodiversitas* 31:153–162
- Hoffeins HW (2001) On the preparation and conservation of amber inclusions in artificial resin. *Pol J Entomol* 70:215–219
- James TY, Kauff F, Schoch CL et al (2006) Reconstructing the early evolution of Fungi using a six-gene phylogeny. *Nature* 443:818–822
- Katoh K, Toh H (2008) Recent developments in the MAFFT multiple sequence alignment program. *Brief Bioinform* 9:286–98
- Knuth G, Koch T, Rappsilber I, Volland L (2002) Concerning amber in the Bitterfeld region—geologic and genetic aspects. *Hallesches Jahrb Geowiss* 24:35–46
- Koponen T, Enroth J, Fang YM, Huttunen S, Hyvönen J, Ignatov M, Juslén A, Lai MJ, Piippo S, Potemkin A, Rao PC (2000) Bryophyte flora of Hunan Province, China, 1. Bryophytes from Mangshan Nature Reserve and Wulingyuan Global Cultural Heritage Area. *Ann Bot Fenn* 37:11–39
- Koponen T, Cao T, Huttunen S, Hyvönen J, Juslén A, Peng C, Piippo S, Rao PC, Vána J, Virtanen V (2004) Bryophyte Flora of Hunan Province, China, 3: Bryophytes from Taoyuandong and Yankou Nature Reserves and Badagongshan and Hupingshan National Nature Reserves, with additions to floras of Mangshan Nature Reserve and Wulingyuan Global Cultural Heritage Area. *Acta Bot Fenn* 177:1–47
- Kumar S, Skjæveland Å, Orr R, Enger P, Ruden T, Mevik BH, Burki F et al (2009) AIR: a batch-oriented web program package for construction of supermatrices ready for phylogenomic analyses. *BMC Bioinforma* 10:357
- Langenheim JH (2003) *Plant resins: chemistry, evolution, ecology and ethnobotany*. Timber Press, Portland
- Müller K, Müller J, Neinhuis C, Quandt D (2010) PhyDE—Phylogenetic Data Editor. www.phyde.de. Retrieved 15 October 2011
- Posada D (2008) jModelTest: Phylogenetic Model Averaging. *Mol Biol Evol* 25:1253–1256
- Pratibha J, Amandeep K, Shenoy BD, Bhat DJ (2011) *Caliciopsis indica* sp. nov. from India. *Mycosphere* 1:65–72
- Ragazzi E, Schmidt AR (2011) Amber. In: Reitner J, Thiel V (eds) *Encyclopedia of Geobiology*. Springer, Dordrecht, pp 24–36
- Rehner S, Samuels GJ (1994) Taxonomy and phylogeny of *Gliocladium* analyzed from nuclear large subunits ribosomal DNA sequences. *Mycol Res* 98:625–634
- Rikkinen J (1999) Two new species of resinicolous *Chaenothecopsis* (Mycocaliciaceae) from western North America. *Bryologist* 102:366–369
- Rikkinen J (2003a) Calicioid lichens and fungi in the forests and woodlands of western Oregon. *Acta Bot Fenn* 175:1–41
- Rikkinen J (2003b) *Chaenothecopsis nigripunctata*, a remarkable new species of resinicolous Mycocaliciaceae from western North America. *Mycologia* 95:98–103
- Rikkinen J, Poinar G (2000) A new species of resinicolous *Chaenothecopsis* (Mycocaliciaceae, Ascomycota) from 20 million year old Bitterfeld amber, with remarks on the biology of resinicolous fungi. *Mycol Res* 104:7–15
- Ronquist F, Huelsenbeck JP (2003) Bayesian phylogenetic inference under mixed models. *Bioinformatics* 19:1572–1574
- Schmidt AR, Dörfelt H (2007) Evidence of Cenozoic Matoniaceae from Baltic and Bitterfeld amber. *Rev Palaeobot Palynol* 144:145–156
- Schmidt AR, Schäfer U (2005) *Leptotrichites resinatus* new genus and species, a fossil sheathed bacterium in alpine Cretaceous amber. *J Paleontol* 79:184–193
- Schmidt AR, Ragazzi E, Coppellotti O, Roghi G (2006) A microworld in Triassic amber. *Nature* 444:835
- Schmidt AR, Jancke S, Lindquist EE, Ragazzi E, Roghi G, Nascimbene P, Schmidt K, Wappler T, Grimaldi DA (2012) Arthropods in amber from the Triassic Period. *PNAS* 109:14796–14801
- Selva SB, Tibell L (1999) Lichenized and non-lichenized calicioid fungi from North America. *Bryologist* 102:377–397
- Standke G (1998) Die Tertiärprofile der Samländischen Bernsteinküste bei Rauschen. *Schriftenr Geowiss* 7:93–133
- Standke G (2008) Bitterfelder Bernstein gleich Baltischer Bernstein?—Eine geologische Raum-Zeit-Betrachtung und genetische Schlussfolgerungen. In: Rascher J, Wimmer R, Krumbiegel G, Schmiedel S (eds) *Bitterfelder Bernstein versus Baltischer Bernstein - Hypothesen, Fakten, Fragen*. Exkursionsführer und Veröffentlichungen der Deutschen Gesellschaft für Geowissenschaften 236:11–33
- Tibell L, Titov A (1995) Species of *Chaenothecopsis* and *Mycocalicium* (Caliciales) on exudate. *Bryologist* 98:550–560
- Tibell L, Vinuesa M (2005) *Chaenothecopsis* in a molecular phylogeny based on nuclear rDNA ITS and LSU sequences. *Taxon* 54:427–442
- Titov A (2001) Further notes on calicioid lichens and fungi from the Gongga Mountains (Sichuan, China). *Lichenologist* 33:303–314
- Titov A (2006) Mikokalizievye griby (porjadok Mycocaliciales) Golarkitki [Mycocalicioid fungi (the order Mycocaliciales) of Holartic]. KMK Scientific Press, Moskva
- Titov A, Tibell L (1993) *Chaenothecopsis* in the Russian Far East. *Nord J Bot* 13:313–329
- Tuovila H, Cobbinah JR, Rikkinen J (2011a) *Chaenothecopsis khayensis*, a new resinicolous calicioid fungus on African mahogany. *Mycologia* 103:610–615
- Tuovila H, Larsson P, Rikkinen J (2011b) Three resinicolous North American species of Mycocaliciales in Europe with a re-evaluation of *Chaenothecopsis oregana* Rikkinen. *Karstenia* 51:37–49
- Vilgalys R, Hester M (1990) Rapid genetic identification and mapping of enzymatically amplified ribosomal DNA from several *Cryptococcus* species. *J Bacteriol* 172:4238–4246
- Vinuesa M, Sanchez-Puelles JM, Tibell L (2001) Intraspecific variation in *Mycocalicium subtile* (Mycocaliciaceae) elucidated by morphology and the sequences of the ITS1-5.8S-ITS2 region of rDNA. *Mycol Res* 105:323–330
- Wang Z, Binder M, Hibbett DS (2005) Life history and systematics of the aquatic discomycete *Mitrula* (Helotiales, Ascomycota) based on cultural, morphological, and molecular studies. *Am J Bot* 92:1565–1574
- Weitschat W (1997) Bitterfelder Bernstein—ein eozäner Bernstein auf miozäner Lagerstätte. *Metalla* 66:71–84
- White TJ, Bruns TD, Lee S, Taylor JW (1990) Amplification and direct sequencing of fungal ribosomal RNA genes for phylogenetics. In: Innis MA, Gelfand DH, Sninsky JJ, White TJ (eds) *CR Protocols: A Guide to Methods and Applications*. Academic, New York, pp 312–322
- Zwickl DJ (2006) Genetic algorithm approaches for the phylogenetic analysis of large biological sequence datasets under the maximum likelihood criterion. Dissertation, The University of Texas